Published online 30 July 2019

Nucleic Acids Research, 2019, Vol. 47, No. 17 **9313–9328**
doi: 10.1093/nar/gkz643

Staufen1 and UPF1 exert opposite actions on the replacement of the nuclear cap-binding complex by eIF4E at the 5′ end of mRNAs

Kwon Jeong[1,2,†], Incheol Ryu[1,2,†], Joori Park[1,2,†], Hyun Jung Hwang[1,2], Hongseok Ha[1,2], Yeonkyoung Park[1,2], Sang Taek Oh[1,2] and Yoon Ki Kim[1,2,*]

[1]Creative Research Initiatives Center for Molecular Biology of Translation, Korea University, Seoul 02841, Republic of Korea and [2]Division of Life Sciences, Korea University, Seoul 02841, Republic of Korea

Received March 25, 2019; Revised July 11, 2019; Editorial Decision July 11, 2019; Accepted July 16, 2019

ABSTRACT

Newly synthesized mRNAs are exported from the nucleus to cytoplasm with a 5′-cap structure bound by the nuclear cap-binding complex (CBC). During or after export, the CBC should be properly replaced by cytoplasmic cap-binding protein eIF4E for efficient protein synthesis. Nonetheless, little is known about how the replacement takes place. Here, we show that double-stranded RNA-binding protein staufen1 (STAU1) promotes efficient replacement by facilitating an association between the CBC–importin α complex and importin β. Our transcriptome-wide analyses and artificial tethering experiments also reveal that the replacement occurs more efficiently when an mRNA associates with STAU1. This event is inhibited by a key nonsense-mediated mRNA decay factor, UPF1, which directly interacts with STAU1. Furthermore, we find that cellular apoptosis that is induced by ionizing radiation is accompanied by inhibition of the replacement via increased association between STAU1 and hyperphosphorylated UPF1. Altogether, our data highlight the functional importance of STAU1 and UPF1 in the course of the replacement of the CBC by eIF4E, adding a previously unappreciated layer of post-transcriptional gene regulation.

INTRODUCTION

In mammalian cells, newly synthesized transcripts by RNA polymerase II (Pol II) undergo various processing steps prior to their export from the nucleus to cytoplasm for polypeptide synthesis (1). The earliest modification is the addition of a cap structure at the 5′ end, which occurs co-transcriptionally while nascent transcripts are being elongated by Pol II. The 5′-cap structure is recognized by the nuclear cap-binding complex (CBC), a heterodimer of cap-binding protein (CBP) 80 and 20 (2,3). The CBC is involved in a wide spectrum of gene expression–regulatory pathways including transcription, pre-mRNA splicing, mRNA stability and the pioneer (or first) round of translation (pioneer translation) (2,4,5).

The fully processed mature mRNAs in the nucleus are exported to the cytoplasm with the 5′ cap bound to the CBC. During or after mRNA export, the CBC is replaced by a cytoplasmic cap-binding protein (eukaryotic translation initiation factor 4E, eIF4E). Both the CBC and eIF4E have a common ability to drive translation initiation by recruiting ribosomes (6–8). Nevertheless, it is generally believed that the pioneer translation driven by the CBC is largely in charge of mRNA surveillance rather than abundant synthesis of polypeptides. When newly synthesized mRNAs contain premature translation termination codons, these aberrant mRNAs are rapidly degraded by the nonsense-mediated mRNA decay (NMD) pathway mostly during pioneer translation (9–12). Otherwise, eIF4E replaces the CBC and allows for multiple rounds of mRNA translation (steady-state translation) to support abundant synthesis of the polypeptide.

Despite the common ability of the CBC and eIF4E to drive translation initiation, CBC-bound messenger ribonucleoproteins (mRNPs) are quite different from eIF4E-bound mRNPs with respect to their composition. For instance, exon junction complexes (EJCs), which are deposited onto mRNAs in the nucleus as a consequence of splicing, are detectable in CBC-bound mRNPs but not in eIF4E-bound mRNPs (6,13). The EJCs in CBC-bound mRNAs are displaced from the mRNAs by an elongating ribosome during pioneer translation (6,13,14).

During pioneer translation, the selective removal of aberrant mRNAs by NMD requires a key NMD factor, UPF1 (11,12). UPF1 is recruited to a terminating ribosome on a premature translation termination codon and induces rapid

*To whom correspondence should be addressed. Tel: +82 232 903410; Fax: +82 292 39923; Email: yk-kim@korea.ac.kr
†The authors wish it to be known that, in their opinion, the first three authors should be regarded as Joint First Authors.

mRNA degradation. During this process, an interaction between CBP80 and UPF1 promotes NMD complex formation (15,16). In addition to the aforementioned UPF1 recruitment to mRNA during translation termination, UPF1 promiscuously binds to mRNAs even before translation according to a recent transcriptome-wide analysis (17) and even associates with nascent RNAs around transcription sites in the nucleus (18). The molecular function of the UPF1 preassociated with mRNA is currently unknown.

In addition to NMD, UPF1 can induce other types of mRNA decay pathways such as staufen (STAU)-mediated mRNA decay (SMD) (12,19,20). When the double-stranded RNA-binding protein STAU binds to the 3′ untranslated region (3′UTR) of an SMD substrate, STAU triggers SMD by recruiting UPF1 in a translation-dependent manner (19,21). Mammalian cells express two STAU paralogs: ubiquitously expressed STAU1 and tissue-specifically expressed STAU2. Besides SMD, STAUs perform multiple functions in post-transcriptional regulatory processes including alternative splicing, translation and spatial targeting of mRNA (22,23).

Although the replacement of the CBC by eIF4E is one of the pivotal steps for gene expression, little is known about the molecular details of this event. Here, we provide molecular evidence that STAU1 and UPF1 act as a positive and a negative cellular regulator, respectively, for the replacement of the CBC by eIF4E. We also show that under stressful conditions induced by ionizing radiation (IR), UPF1 is hyperphosphorylated and attenuates the ability of STAU1 to promote this replacement. Furthermore, the level of UPF1 phosphorylation correlates with the efficiency of cellular apoptosis. Thus, our results reveal previously unappreciated roles of STAU1 and UPF1 in the replacement of the CBC by eIF4E, thereby highlighting the biological importance of proper replacement.

MATERIALS AND METHODS

Plasmid construction

The following constructs have been described in previous studies: No intron and 5′ intron (24); SL-No intron and SL-5′ intron (25); No intron-MS2bs (originally named as 'RLuc-8bs'), pMS2-HA-MBP and pHA-MBP (26); pMS2-HA and pcDNA3-human $STAU1^{55}$-HA_3 (19); pCMV-Myc-$UPF1^R$ and pCMV-Myc-$UPF1^R$-HP (27); pCMV-Myc-$UPF1^R$-4SA (28); pRL-CMV-5′-5BoxB, pCI-FLuc, pλN-HA and pλN-HA-GFP (29); pcDNA3-FLAG-$UPF1^R$ (30); pcDNA3.1-HA and pCMV-Myc-STAU1 (31); pCI-neo-STAU1(A375E/R376A/L472S/S473E)-FLAG (32); pcDNA3-FLAG and pcDNA3-FLAG-CBP80 (7); pEGFP-C2 and pCMV-Myc (Clontech); and pGL3-control (Promega). pCMV3-IMPβ-FLAG encoding full-length human *IMPβ1* cDNA (GenBank accession No. NM_001276453.1) with the FLAG tag at the C terminus was purchased from Sino Biological Inc. (Beijing, China).

To construct pcDNA3.1-CBP80-HA, a DNA fragment containing human *CBP80* cDNA was amplified by polymerase chain reaction (PCR) using pcDNA3-FLAG-CBP80 as a template and two specific oligonucleotides: 5′-CTAGCTAGCGCCACCATGTCGCGGCGGCGGCACAGCGACGAGA-3′ (sense) and 5′-CCGCTCGAGCGGCCTGCAGGGCACAGAACTGCTGGAACA-3′ (antisense), where the underlined nucleotides specify the NheI and XhoI sites, respectively. The PCR-amplified fragment was ligated to linearized pcDNA3.1-HA digested with NheI and XhoI.

To construct pcDNA3-FLAG-GFP, GFP cDNA was amplified by PCR with pEGFP-C2 as a template and two specific oligonucleotides: 5′-CGGGATCCGCTCGAGATGGTGAGCAAGGGCGAGGAGCTGTTC-3′ (sense) and 5′-CCCAAGCTTGCGGCCGCCTACTTGTACAGCTCGTCCATGCCGAGAGTG-3′ (antisense), where the underlined sequences denote BamHI and HindIII, respectively. The PCR-amplified fragment was ligated to linearized pcDNA3-FLAG digested with BamHI and HindIII.

To generate pλN-HA-STAU1-wild type (WT), a SalI/Klenow-filled NotI fragment of pCMV-Myc-STAU1 was ligated to a XhoI/Klenow-filled NotI fragment of pλN-HA.

To construct pλN-HA-STAU1-Mut encoding the STAU1 mutant that fails to interact with UPF1, a XbaI/NotI fragment of pλN-HA was ligated to two DNA fragments: First, the 5′ fragment was obtained from pλN-HA-STAU1-WT, which was digested with XbaI and EcoRI. Second, the 3′ fragment was amplified by PCR using pCI-neo-STAU1(A375E/R376A/L472S/S473E)-FLAG as a template and two specific oligonucleotides: CCTGCTGGAATTCTTCCCATGGTG-3′ (sense) and AAAGCGGCCGCTTAGCACCTCCCACACACAGACATTGG-3′ (antisense), where the underlined sequences specify EcoRI and NotI sites, respectively.

For construction of pλN-HA-$UPF1^R$, a XhoI/Klenow-filled Acc65I fragment of pMS2-HA-$UPF1^R$ and an Acc65I/NotI fragment of pCMV-Myc-$UPF1^R$ were ligated to an EcoRI/Klenow-filled NotI fragment of pλN-HA.

For the construction of SL-No intron-MS2bs, a fragment of the strong stem-loop (SL) structure obtained from a HindIII-digested SL-No intron was ligated to a HindIII fragment of No intron-MS2bs.

All PCRs in our study were carried out using the Advantage-HF2 PCR Kit (Clontech). All the constructs were verified by DNA sequencing.

Cell culture and transfection

HeLa and HEK293T cells were maintained in Dulbecco's modified Eagle's medium (Capricorn Scientific) supplemented with 10% (v/v) of fetal bovine serum (Capricorn Scientific) and 1% (v/v) of a penicillin/streptomycin solution (Capricorn Scientific). The cells were transiently transfected as previously described (28,33–35). Briefly, for immunoprecipitation (IP) and RNA-IP experiments on HEK293T cells, the calcium phosphate method was employed for DNA transfection. Otherwise, Lipofectamine 2000 (Life Technologies) was utilized for transfection of a reporter plasmid. For small interfering RNA (siRNA) transfection, 100 μM *in vitro*-synthesized siRNAs (GenePharma) were introduced into cells by means of either Oligofectamine (Life Technologies) or Lipofectamine 3000 (Life Technologies).

The following siRNA sequences were used for specific downregulation of endogenous proteins: 5′-r(GAUG CAGUUCCGCUCCAUU)d(TT)-3′ (*UPF1* siRNA), 5′-r(GGCUUUUGUCCCAGCCAUC)d(TT)-3′ (*UPF2* siRNA), 5′-r(CAGAGAGGCUGGAGGUGAA)d(TT)-3′ (*STAU1* siRNA), 5′-r(CGAGCAAUCAAGCAGA UCA)d(TT)-3′ (*eIF4A3* siRNA), 5′-r(UCCAGCCU UCAACAGAGCG)d(TT)-3′ (*Y14* siRNA), and 5′-r(ACAAUCCUGAUCAGAAACC)d(TT)-3′ (a nonspecific control siRNA).

For exposure to ionizing radiation (IR), 2 days after transfection, the cultured cells were γ-irradiated with a ^{137}Cs source (10 Gy; IBL-437C, CIS bio International) and then were subjected to RNA-IP, a surface sensing of translation (SUnSET) assay or the terminal deoxynucleotidyl transferase dUTP nick end labeling (TUNEL) assay.

Immunoprecipitation, the MBP pull-down assay and nuclear and cytoplasmic fractionation

IP and RNA-IP were performed on HEK293T cells as previously described (28,33–35). MBP pull-down assays were conducted as described elsewhere (25). In case of RNA-IP, equal amounts of *in vitro*-synthesized firefly luciferase (FLuc) RNAs were added to the samples (after IP) as a spike-in (10 pg per sample). The samples either before or after IP were subjected to Western blotting or quantitative reverse-transcription PCR (qRT-PCR). For IPs in the cytoplasmic fraction, the nuclear fraction and cytoplasmic fraction were separated, as described previously (6).

Western blotting

Antibodies against the following proteins were used for IPs and Western blots: CBP80 (36), eIF4E (610269, BD Bioscience; 2067, Cell Signaling Technology), UPF1 (a gift from Lynne E. Maquat), phospho-(S/T)Q (2851, Cell Signaling Technology), UPF2 (36), STAU1 (A303–956A, Bethyl Laboratories), IMPα (A300–484A, Bethyl Laboratories), PABPN1 (A303–524A, Bethyl Laboratories), eIF4A3 [sc-365549, Santa Cruz Biotechnology; (36)], Y14 (MAB2484, Abnova), p53 (2524, Cell Signaling Technology), phospho-Ser15-p53 (9284, Cell Signaling Technology), U1 snRNP70 (sc-390899, Santa Cruz Biotechnology), FLAG (A8592, MilliporeSigma), HA (11 867 431 001, Roche), Myc (OP10L, Calbiochem), β-actin (A5441, MilliporeSigma), and GAPDH (LF-PA0212, Ab Frontier). For IP of endogenous eIF4E, we employed an in-house anti-eIF4E antibody, which was raised in rabbits against a human eIF4E-specific peptide (MATVEPETTPTPNPPTTE EEKTESNQEVANPEHYIKH).

Signal intensities of Western blot bands were quantitated in the Image J software (version 1.5, National Institutes of Health).

A SUnSET assay

This assay was performed as described previously (37). Briefly, HeLa cells were pulsed with 10 μg/ml puromycin (MilliporeSigma) for 30 min before harvesting. The cytoplasmic extracts were resolved by SDS-PAGE, transferred to a nitrocellulose membrane, and subjected to Western blotting using an anti-puromycin antibody (MABE343, MilliporeSigma). The band intensities in Western blots were normalized to those obtained by Ponceau S (MilliporeSigma) staining before the Western blotting.

Quantitative real-time PCR (qRT-PCR) analysis

Total-RNA samples were isolated using the TRIzol Reagent (Life Technologies). Complementary DNAs (cDNAs) were prepared as previously described (28,33–35). qRT-PCR analysis was conducted with gene-specific oligonucleotides (Supplementary Table S1) and the Light Cycler 480 SYBR Green I Master Mix (Roche) on a Light Cycler 480 II machine (Roche). The qRT-PCR analysis was performed according to the MIQE guideline (38).

A dual luciferase assay

Renilla luciferase (RLuc) and FLuc activities were measured by means of the Dual Luciferase Assay Kit (Promega).

An *in vitro* replacement assay

For preparation of a FLAG-tagged fusion protein, either FLAG-GFP or IMPβ-FLAG, HEK293T cells were transiently transfected with a plasmid expressing either FLAG-GFP or IMPβ-FLAG. Two days later, the FLAG-tagged fusion protein was immunopurified using anti-FLAG antibody-conjugated agarose beads (MilliporeSigma) and eluted with 3×FLAG peptides (MilliporeSigma) as described elsewhere (25).

For preparation of CBC-bound mRNPs, HEK293T cells were transfected with either *STAU1* siRNA or nonspecific control siRNA. One day later, the cells were transfected with a plasmid expressing SL-5′ intron mRNA. Two days later, the cells were harvested and subjected to RNA-IP with either nonspecific rabbit IgG (rIgG) or an anti-CBP80 antibody incubated with protein A Dynabeads (Invitrogen) for 3 h at 4°C. After incubation, the beads were washed five times with NET-2 buffer [50 mM Tris (pH 7.4), 150 mM NaCl, 1 mM phenylmethylsulfonyl fluoride, 2 mM benzamidine hydrochloride and 0.05% NP-40] containing 100 U/ml RNase inhibitor (Thermo Fisher Scientific). After that, the bead-bound RNAs and proteins were resuspended in NET-2 buffer and mixed with the eluted FLAG-tagged fusion protein (either FLAG-GFP or IMPβ-FLAG) for 15 min at 37°C. After centrifugation, the bead-bound RNAs were mixed with spike-in FLuc RNA and were analyzed further.

The TUNEL assay

This assay was conducted with the *in situ* cell death detection kit (12156792910, Roche) as described previously (33). In brief, HeLa cells transiently overexpressing λN-HA-GFP, λN-HA-STAU1-WT or λN-HA-STAU1-Mut were either not treated or exposed to IR (10 Gy). Twelve hours after IR exposure, the cells were fixed in phosphate-buffered saline (PBS) containing 4% paraformaldehyde for 30 min at

room temperature (RT). To block endogenous peroxidase activity, the cells were incubated in PBS containing 3% of hydrogen peroxide (MilliporeSigma) for 10 min at RT. The cells were permeabilized with 0.1% Triton X-100 in PBS for 10 min at RT. Then, single- and double-stranded DNA breaks, a hallmark of the early stages of apoptosis, were labeled with tetramethylrhodamine red for 1 h at 37°C. Nuclei were stained with 4′,6-diamidino-2-phenylindole (DAPI; Biotium) for 5 min at RT. The stained cells were visualized by means of a confocal microscope (LSM 700 or 800, Carl Zeiss). For the quantification of apoptotic cells, more than 100 cells were analyzed for each experiment. The results obtained from three independently performed transfection experiments and TUNEL assays were quantified and analyzed.

QuantSeq 3′-mRNA sequencing

Coimmunoprecipitated transcripts in the IPs of CBP80 or of eIF4E (from the cytoplasmic extracts of HeLa cells) were isolated using the TRIzol Reagent. RNA quality was assessed on an Agilent 2100 bioanalyzer with the RNA 6000 Nano Chip (Agilent Technologies), and RNA quantification was conducted on an ND-2000 Spectrophotometer (Thermo Scientific). Library construction was performed using the QuantSeq 3′ mRNA-Seq Library Prep Kit (Lexogen). Briefly, reverse transcription was carried out using an oligo-dT primer containing an Illumina-compatible sequence at its 5′ end. After removal of the RNA template, the second strand was synthesized via a random primer containing an Illumina-compatible linker sequence at its 5′ end. The double-stranded library was purified on magnetic beads and then amplified to add the complete adapter sequences required for cluster generation. The amplified library was purified and subjected to high-throughput sequencing as single-end (1 × 75 bp) reads on NextSeq 500 (Illumina).

Data analysis

QuantSeq 3′ mRNA-Seq reads were aligned to a reference human genome (hg19) in Bowtie2 (39). For the alignment to the genome and transcriptome, Bowtie2 indexes were generated either from the genome assembly sequence or from representative transcript sequences. Differentially expressed genes were analyzed on the basis of the counts obtained from unique and multiple alignments by means of the coverage in Bedtools (40).

Cumulative distribution function analysis was performed by comparing the relative ratios of mRNAs enriched in the IPs of CBP80 and eIF4E. To examine STAU1 dependence, mRNAs were categorized into two groups (non-targets and STAU1 targets), based on the previously published microarray data for mRNAs enriched in the IP of STAU1 (GSE8438) (41).

Statistical analysis

Throughout the paper, quantitative data are shown as the means ± SD from at least three independently conducted experiments. Statistical analyses were performed by two-tailed, equal-variance Student's *t*-test. In all cases, statistical significance was presumed at a P-value < 0.05. For cumulative distribution analysis, the P-value was calculated by the two-tailed Mann–Whitney U-test.

RESULTS

A translation event and EJCs are dispensable for efficient replacement of the CBC by eIF4E

As the first step toward elucidation of the molecular basis for CBC replacement by eIF4E, we tested whether this replacement is dependent on translation and/or EJCs. To this end, we employed three reporter plasmids (Figure 1A): (i) 'No intron,' which encodes an intronless RLuc gene with exons 6 and 7 from the human triose phosphate isomerase (*TPI*) gene at both ends, (ii) an inefficiently translated reporter mRNAs lacking an intron, 'SL-No intron,' which contains an SL structure ($\Delta G = -87.8$ kcal/mol) in the middle of the 5′UTR of the No intron reporter and (iii) an inefficiently translated reporter mRNAs harboring an intron, 'SL-5′ intron,' which contains both the SL in the 5′UTR and *TPI* intron 6 between exons 6 and 7 of *TPI* upstream of the RLuc gene. The last two reporter plasmids were expected to express identical mRNAs with respect to nucleotide sequences. Although SL-No intron mRNA should lack an EJC, SL-5′ intron mRNA is likely to have one EJC as a consequence of splicing of the *TPI* intron. Additionally, studies have shown that the presence of an SL in the 5′UTR blocks ribosome scanning through the 5′UTR, resulting in drastic inhibition of translation (25,29,35). As expected, relative translation efficiency of the reporter RLuc mRNA was strongly reduced by the presence of the SL in the 5′UTR (Supplementary Figure S1A). In addition, consistently with previous reports showing that EJCs are displaced from an mRNA by an elongating ribosome (6,13,14), we observed that the presence of an SL in the 5′UTR increased the amount of mRNA-bound EJCs (Supplementary Figure S1B–H).

Next, we carried out IP experiments using either the anti-CBP80 or anti-eIF4E antibody in the cytoplasmic extracts of cells expressing one of the reporter mRNAs. It is possible that a difference in the export efficiency of reporter mRNAs may indirectly affect replacement efficiency. To minimize the indirect effect, therefore, we carried out IP experiments in the cytoplasmic extracts. Proper nuclear and cytoplasmic separation was confirmed by monitoring the distribution of cellular U1 snRNP70 and GAPDH, a nuclear protein and cytoplasmic protein, respectively (Supplementary Figure S1I). In addition, it was confirmed by qRT-PCRs that the amounts of input reporter mRNAs were comparable (Supplementary Figure S1J). Furthermore, we observed that CBP80, but not eIF4E, was detectably enriched in the IP of CBP80 and *vice versa* (Figure 1B), indicating specificity of the IPs under our conditions and a lack of eIF4E in CBP80-associated mRNPs and *vice versa*. After IPs, *in vitro*-synthesized FLuc RNA was added to the immunoprecipitated samples as a spike-in control to adjust the data for differences among RNA preparations. Then, the relative amounts of coimmunoprecipitated (co-IPed) reporter mRNAs were measured by qRT-PCRs.

The IP results revealed that, in line with some studies showing preferential enrichment of replication-dependent

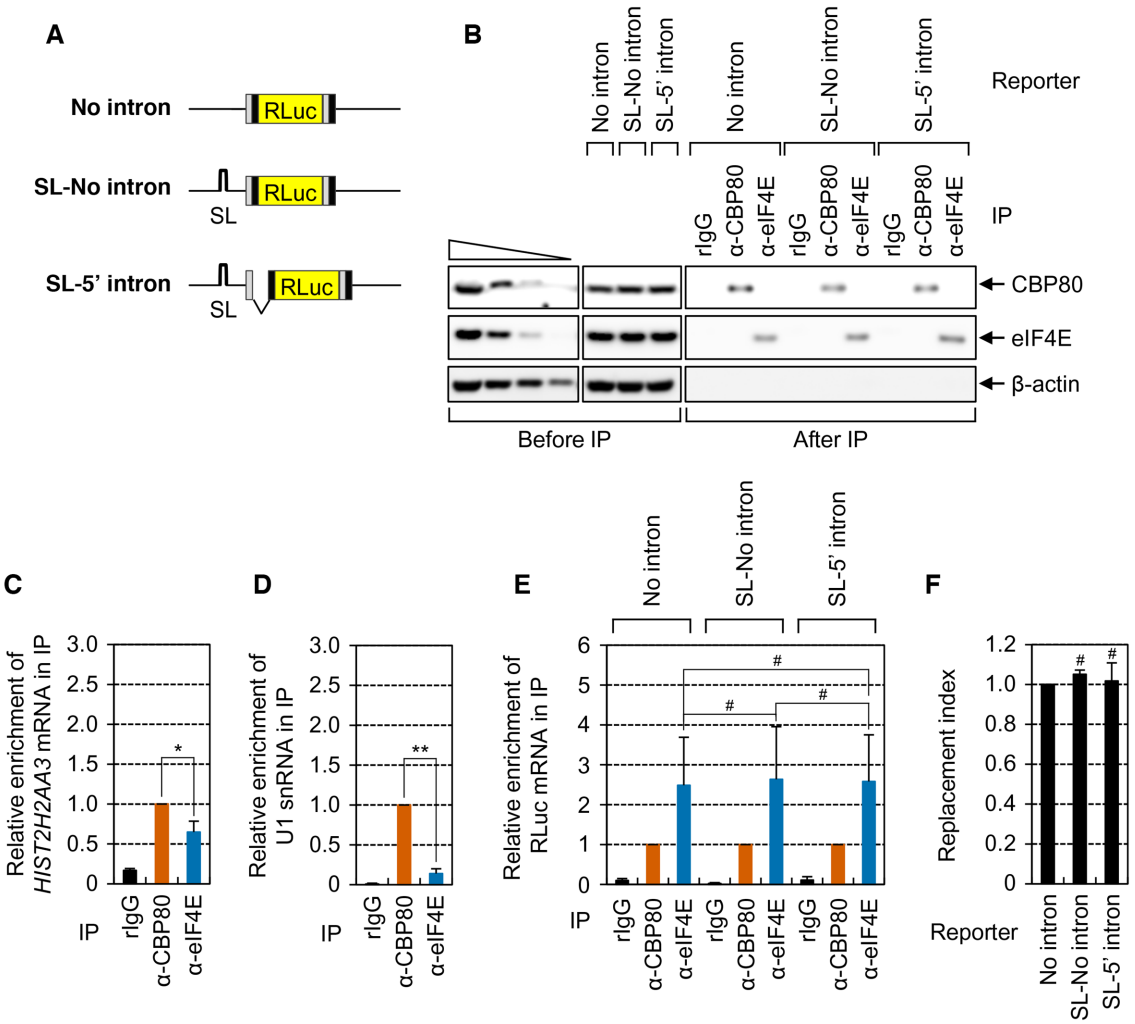

Figure 1. Translation and the EJC are not involved in efficient replacement of the CBC by eIF4E. (**A**) A schematic diagram of RLuc reporter mRNAs. RLuc, *Renilla* luciferase; SL, a stem-loop structure. (**B**–**F**) The efficiency of replacement of the reporter mRNAs. HEK293T cells were transiently transfected with one of RLuc reporter plasmids. The cytoplasmic extracts were subjected to IP experiments with the anti-CBP80 or anti-eIF4E antibody or with non-specific rabbit IgG (rIgG). Then, equal amounts of *in vitro*-synthesized FLuc RNAs were added to the samples after IP as a spike-in, which served as a control to adjust the data for variation among the RNA samples. Two-tailed equal-variance Student's *t* test was carried out for statistical analysis. Data were obtained from three independent experiments ($n = 3$). *, $P < 0.05$; **, $P < 0.01$; $^{\#}$, not significant. (B) IPs of either endogenous CBP80 or eIF4E from the cytoplasmic extracts. The protein samples before or after IPs were analyzed by Western blotting. To demonstrate that Western blots were semiquantitative, the cytoplasmic extracts serially diluted 3-fold were loaded in the four leftmost lanes. (C) Relative levels of co-IPed endogenous *HIST2H2AA3* mRNAs normalized to those of endogenous β-actin mRNAs. The normalized level of co-IPed endogenous *HIST2H2AA3* mRNAs in the IP of CBP80 was arbitrarily set to 1.0. (D) Relative levels of co-IPed endogenous U1 snRNA normalized to spike-in RNA. (E) Relative levels of co-IPed reporter mRNAs. The normalized levels of co-IPed reporter mRNAs in each IP of CBP80 were arbitrarily set to 1.0. (F) The replacement index of the RLuc reporter mRNAs. Replacement indices were determined by normalizing the relative levels of co-IPed reporter mRNAs in the IP of eIF4E to those in the IP of CBP80.

histone mRNAs and U1 small nuclear RNA (snRNA) in the IP of cytoplasmic CBP80 (42,43), a greater amount of those mRNAs turned out to be enriched in the IP of CBP80 relative to the IP of eIF4E (Figure 1C and D). In the same IPs, comparable amounts of all the tested reporter mRNAs were found to be enriched in the IPs of either CBP80 or eIF4E (Figure 1E). Furthermore, the relative levels of co-IPed reporter mRNAs in the IP of eIF4E normalized to those in the IP of CBP80 (hereafter, this value is referred to as the replacement index) were not significantly different among the tested reporter mRNAs (Figure 1F). Therefore, all the data indicate that the replacement of the CBC by eIF4E at the cap of canonical poly(A)-containing mRNAs is not dependent on translation and occurs independently of the presence of introns (that is, EJCs). In support of these conclusions, the relative levels of co-IPed SL-5′ intron mRNA and the replacement index were not significantly affected when the cells were depleted of an EJC component (eIF4A3 or Y14; Supplementary Figure S2). The translation-independent replacement of the CBC by eIF4E was further demonstrated by RNA pull-down experiments involving maltose-binding protein (MBP) followed by Western blotting (Supplementary Figure S3).

UPF1 inhibits the replacement of the CBC by eIF4E

What cellular factor(s) participates in the replacement of the CBC by eIF4E? Given that (i) UPF1 promiscuously associates with mRNAs even before translation (17,18) and (ii) UPF1 preferentially binds to the CBC of newly synthesized mRNAs (15,16), we first tested whether the replacement involves UPF1. To this end, we carried out IPs of CBP80 or eIF4E in the cytoplasmic extracts of the cells that transiently expressed SL-5′ intron mRNAs and were either undepleted or depleted of UPF1. Because the CBC replacement by eIF4E is independent of a translation event (Figure 1), we used the SL-5′ intron mRNA hereafter throughout the experiments to exclude a possible indirect effect of translation on the replacement.

Comparable IPs of CBP80 and eIF4E, specific downregulation of endogenous UPF1 by siRNA, proper nuclear and cytoplasmic separation, and comparable expression of the reporter mRNAs were all confirmed by Western blotting (Supplementary Figure S4A–D). The IP results revealed that UPF1 downregulation decreased and increased the relative amounts of SL-5′ intron mRNAs in the IP of CBP80 and eIF4E, respectively (Figure 2A and B), and increased the replacement index 3.5-fold (Figure 2C), meaning that UPF1 functions as a negative regulator of the replacement.

STAU1 serves as a positive regulator of the replacement of the CBC by eIF4E

We next determined whether the UPF1-mediated inhibition of the replacement is affected by previously known UPF1-interacting proteins (UPF2 and STAU1). In agreement with the EJC-independent replacement of the CBC by eIF4E (Figure 1 and Supplementary Figure S2), downregulation of UPF2 (a peripheral EJC component) did not significantly affect the relative levels of co-IPed SL-5′ intron mRNA and the replacement index (Supplementary Figure S4E–J). In contrast, the downregulation of STAU1 yielded the results opposite to those obtained after UPF1 downregulation (Figure 2A–C), indicating that STAU1 promotes the replacement of the CBC by eIF4E.

To assess the transcriptome-wide influence of STAU1 on the replacement, we applied QuantSeq 3′-mRNA sequencing (QuantSeq) to co-IPed RNAs obtained from IPs of CBP80 or eIF4E in the cytoplasmic extracts of HeLa cells either undepleted or depleted of STAU1. Pearson correlation coefficients between reads per million reads (RPM) values were above 0.845 (Supplementary Table S2), pointing to a strong correlation between the two biological replicates of each IP. A scatter plot of QuantSeq data showed that the majority of cellular mRNAs co-IPed at comparable ratios with CBP80 relative to eIF4E in the cells either undepleted (Supplementary Figure S4K) or depleted (Supplementary Figure S4L) of STAU1. Next, we compared the relative change in the replacement index between two groups of mRNAs after STAU1 downregulation: non-targets and STAU1 targets. The lists of mRNAs either associated (STAU1 targets, 573 mRNAs) or not associated (non-targets, 8949 mRNAs) with STAU1 were obtained from previously performed RNA-IP followed by microarray analysis of STAU1 (41). The cumulative distribution function analysis showed that the replacement index of STAU1 targets significantly decreased when the cells were depleted of STAU1 (Figure 2D, $P = 1.2 \times 10^{-4}$, two-tailed Mann–Whitney *U*-test), indicating that STAU1 acts as a positive regulator of the replacement of the CBC by eIF4E at the transcriptome-wide level. The calculated replacement indices of each mRNA are summarized in Supplementary Table S3.

UPF1 downregulation promotes an association between STAU1 and IMPα–CBC-capped mRNA

As shown in an X-ray crystallographic study (44), the capped mRNA-bound CBC is complexed with importin α (IMPα). In the cytosol, IMPβ binds to the IMPα–CBC-capped mRNA complex and triggers the release of capped mRNA through GTP hydrolysis. The released capped mRNA associates with eIF4E. The remaining IMPβ–IMPα–CBC complex enters the nucleus and is separated into IMPβ and the IMPα–CBC complex by the action of GTP-bound Ran. Then, the IMPα–CBC complex binds to the cap of newly synthesized RNAs, again forming the IMPα–CBC-capped mRNA complex. Of note, it is known that the IMPβ-mediated replacement of the CBC by eIF4E occurs in a translation-independent manner (43).

Which steps of the CBC cycle are targeted by UPF1 and STAU1? Our IP data showed that comparable amounts of endogenous IMPα were enriched in the IPs of CBP80-HA in a manner that was resistant to digestion with RNase A and independent of either UPF1 or STAU1 downregulation (Figure 3A). On the contrary, a greater amount of endogenous STAU1 co-IPed with CBP80-HA after downregulation of UPF1 in an RNase A-resistant manner (Figure 3B). We also observed that ∼2-fold more CBP80 and IMPα were enriched in the IP of the C-terminally HA-tagged STAU1[55], which is the most abundant form of STAU1 (22), in an RNase A-resistant manner after UPF1 downregulation (Figure 3B). All these data indicate that (i) the interaction between the CBC and IMPα is not affected by UPF1 and STAU1 and (ii) UPF1 downregulation promotes the binding of STAU1 to the IMPα–CBC-capped mRNA complex.

STAU1 facilitates efficient recruitment of IMPβ to IMPα–CBC-capped mRNA, thus, triggering dissociation of capped mRNA

Because an interaction between the CBC and IMPα is not affected by STAU1 (Figure 3A), we hypothesized that STAU1 has an influence on an interaction of IMPβ with the IMPα–CBC-capped mRNA complex for CBC replacement by eIF4E. Indeed, STAU1 downregulation reduced the levels of co-IPed CBP80 and IMPα in the IP of IMPβ-FLAG (Figure 4A), indicating that STAU1 facilitates the association between IMPβ and the IMPα–CBC-capped mRNA complex.

To further corroborate the above findings, we established an *in vitro* replacement assay system (Figure 4B). Either overexpressed IMPβ-FLAG or, as a control, FLAG-tagged green fluorescent protein (FLAG-GFP) in HEK293T cells was immunopurified by IPs using anti-FLAG antibody–conjugated agarose beads followed by elution using FLAG

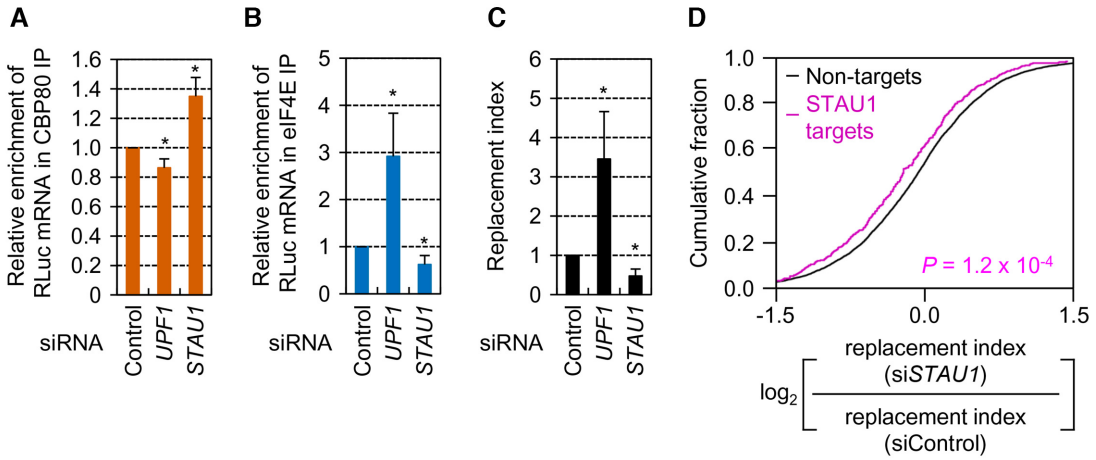

Figure 2. Downregulation of UPF1 or STAU1, respectively, promotes or inhibits the replacement. (**A**–**C**) The effect of UPF1 or STAU1 downregulation on the replacement. IPs of either CBP80 or eIF4E were carried out in the cytoplasmic extracts of HEK293T cells that transiently expressed SL-5′ intron RLuc reporter mRNAs and were either undepleted or depleted of UPF1 or STAU1; $n = 3$; *, $P < 0.05$. (A) Relative levels of co-IPed RLuc reporter mRNAs in the IPs of CBP80. (B) Relative levels of co-IPed RLuc reporter mRNAs in the IPs of eIF4E. (C) The replacement index of the RLuc reporter mRNAs. (**D**) Cumulative distribution functions for the change in the relative ratio of the replacement index in STAU1-depleted cells relative to undepleted cells between non-targets and STAU1 targets. The *P*-value was calculated by the two-tailed Mann–Whitney *U*-test ($n = 2$).

peptides. In parallel, CBC-associated RLuc mRNPs were immunopurified by IPs with the anti-CBP80 antibody in the extracts of cells that expressed SL-5′ intron mRNAs and were either undepleted or depleted of endogenous STAU1. Specific immunopurification and downregulation were confirmed by Western blotting (Supplementary Figure S5). Then, *in vitro* replacement assays were performed by mixing either immunopurified FLAG-GFP or IMPβ-FLAG with the agarose beads bound to immunopurified CBC-associated mRNPs. After the reaction, the remaining RLuc mRNA on the agarose beads was quantitated by qRT-PCRs.

The results showed that the addition of immunopurified IMPβ-FLAG reduced by 56% of the amount of agarose bead-bound RLuc mRNA immunopurified from undepleted cells (Figure 4C), thus pointing to efficient dissociation of mRNA from the IMPα–CBC-capped mRNA complex by IMPβ in our system. In contrast, the amount of agarose bead-bound RLuc mRNA immunopurified from STAU1-depleted cells was not significantly changed by the addition of immunopurified IMPβ-FLAG, compared to immunopurified FLAG-GFP (Figure 4D). Collectively, these data indicate that STAU1 facilitates the recruitment of IMPβ, consequently, leading to efficient dissociation of capped mRNA from the IMPα–CBC-capped mRNA complex by IMPβ.

Artificial tethering of STAU1 or UPF1, respectively, promotes or inhibits the replacement of the CBC by eIF4E

To validate the functions of STAU1 and UPF1 in the replacement, we employed an artificial tethering system: the bacteriophage λN-5BoxB system. The reporter RLuc-5′-5BoxB mRNA contained five tandem repeats of a BoxB sequence (5BoxB), which is a specific *cis*-acting element for the binding of the bacteriophage λN protein, in the 5′UTR of the intronless RLuc gene (Figure 5A). The FLuc mRNA lacking 5BoxB served as a control to adjust the data for variations of transfection and RNA preparation. The replacement efficiency was determined by comparing the relative levels of co-IPed RLuc reporter mRNAs normalized to the levels of co-IPed FLuc mRNAs in the IPs of either CBP80 or eIF4E in the cytoplasmic extracts of cells transiently expressing one of effector proteins: λN-HA-GFP, λN-HA-UPF1 or λN-HA-STAU1 (Figure 5B–D). Reliable separation of nuclear and cytoplasmic fractions, comparable expression levels of effector proteins, and specific IPs of CBP80 or eIF4E were confirmed by Western blotting (Supplementary Figure S6A–C).

The results showed that, although the abundance of RLuc reporter mRNAs before IPs was not significantly affected by effector protein expression (Figure 5B), the amounts of co-IPed RLuc reporter mRNAs in the CBP80 IP increased 1.5-fold or decreased by 23% when λN-HA-UPF1 or λN-HA-STAU1 was tethered, respectively (Figure 5C, compare lanes 3 and 5). In contrast, the level of co-IPed RLuc reporter mRNAs in the IP of eIF4E significantly decreased (by 47%) or increased 3.1-fold when λN-HA-UPF1 or λN-HA-STAU1 was tethered, respectively (Figure 5C, compare lanes 4 and 6). U1 snRNA, which is known to exclusively associate with the CBC (45), preferentially coimmunopurified with CBP80 rather than with eIF4E (Supplementary Figure S6D), confirming the specificity of IPs. Thus, all our data indicate that UPF1 and STAU1 function as a negative and positive regulator, respectively, of the CBC replacement by eIF4E.

Because the translation driven by eIF4E is more efficient than that driven by the CBC (6,7), the change in the replacement efficiency might be reflected in translation efficiency. In agreement with this notion, the relative level of cytoplasmic RLuc protein activity decreased by 37% or increased by 2.7-fold when λN-HA-UPF1 or λN-HA-STAU1 was tethered, respectively, without a significant influence on the relative levels of cytoplasmic RLuc mRNA (Figure 5D).

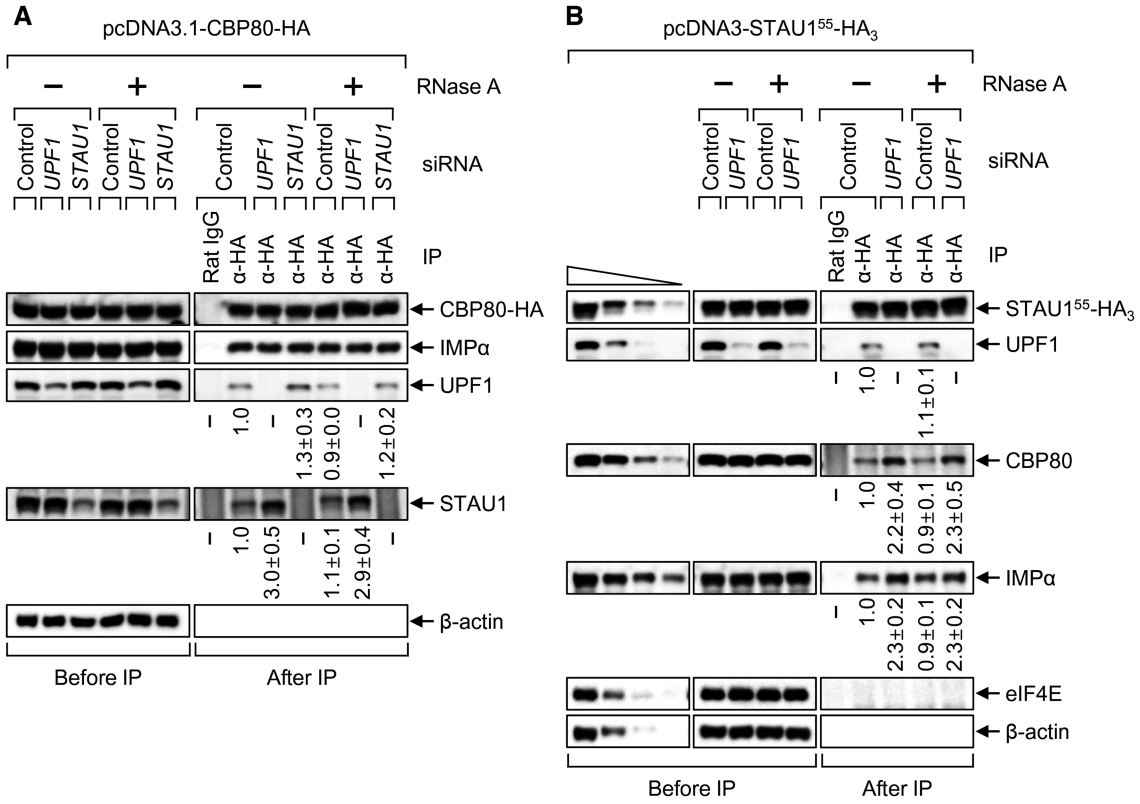

Figure 3. UPF1 downregulation increases an association between STAU1 and the IMPα–CBC-capped mRNA complex. (**A**) IPs of CBP80-HA. HEK293T cells depleted of either UPF1 or STAU1 were transiently transfected with a plasmid expressing CBP80-HA. The cytoplasmic extracts were either untreated or treated with RNase A and subjected to IP using either an anti-HA antibody or a nonspecific rat IgG. The relative levels of co-IPed proteins were calculated by normalizing the intensities of the bands to those of immunoprecipitated CBP80-HA. The normalized level from the cells undepleted and not treated with RNase A was arbitrarily set to 1.0. $n = 2$. (**B**) IPs of STAU1^{55}-HA$_3$. As performed in panel A, except that HEK293T cells depleted of UPF1 were transiently transfected with a plasmid expressing STAU1^{55}-HA$_3$. $n = 2$.

The ability of STAU1 to promote the replacement of the CBC by eIF4E is inhibited via an interaction of STAU1 with UPF1

How do UPF1 and STAU1 exert the opposite actions on the replacement of the CBC by eIF4E? Considering that STAU1 is known to directly interact with UPF1 (19,32), the ability of STAU1 to promote the replacement may be attenuated by its direct interaction with UPF1. To test this possibility, we generated λN-HA-STAU1-Mut (Figure 5A), which contained four point mutations—A375E, R376A, L472S, and S473E—and lost the UPF1-binding ability (32). Disruption of the interaction between STAU1 and UPF1 by the mutation was confirmed by IPs under our conditions (Supplementary Figure S6E).

Using λN-HA-STAU1-WT and λN-HA-STAU1-Mut, we conducted the same tethering experiments and measured the replacement efficiency. Reliable nuclear and cytoplasmic fractionation, comparable expression levels of effector proteins, and specificity of the IPs were all evidenced by Western blotting (Supplementary Figure S6F–H). The relative amount of RLuc reporter mRNAs was not significantly influenced by effector protein expression before IPs (Figure 5E). On the other hand, tethered λN-HA-STAU1-WT or λN-HA-STAU1-Mut caused a 26% or 47% reduction in the amounts of co-IPed RLuc reporter mRNAs in the IPs of CBP80, respectively (Figure 5F, compare lanes 3 and 5). Conversely, 2.2-fold or 4.8-fold more RLuc reporter mRNAs were enriched in the IPs of eIF4E when λN-HA-STAU1-WT or λN-HA-STAU1-Mut was tethered, respectively (Figure 5F, compare lanes 4 and 6). The preferential enrichment of the U1 snRNA in the IPs of CBP80 was not affected by effector protein expression (Supplementary Figure S6I). In addition, the increase in the replacement efficiency by tethered λN-HA-STAU1-Mut was reflected in increased translation efficiency of RLuc reporter mRNAs (Figure 5G). All these data indicate that UPF1 inhibits the ability of STAU1 to promote the replacement of the CBC by eIF4E via its direct interaction with STAU1.

In our tethering experiments, the level of RLuc-5′-5BoxB mRNA, which was normalized to that of FLuc mRNA, was preferentially affected by tethered UPF1 or STAU1. Nonetheless, these observations do not mean that an mRNA lacking 5BoxB is insensitive to the expressed UPF1 or STAU1. In particular, our finding that UPF1 downregulation promotes an association between STAU1 and IMPα–CBC-capped mRNA in an RNase A-resistant manner (Figure 3) indicates that the replacement of the CBC by eIF4E is in part dependent on protein–protein interactions. In support of this notion, overexpression of λN-HA-UPF1 or λN-HA-STAU1 increased or decreased, respectively, the amount of co-IPed SL-5′ intron mRNAs lacking 5BoxB in the IPs of CBP80 (Supplementary Figure

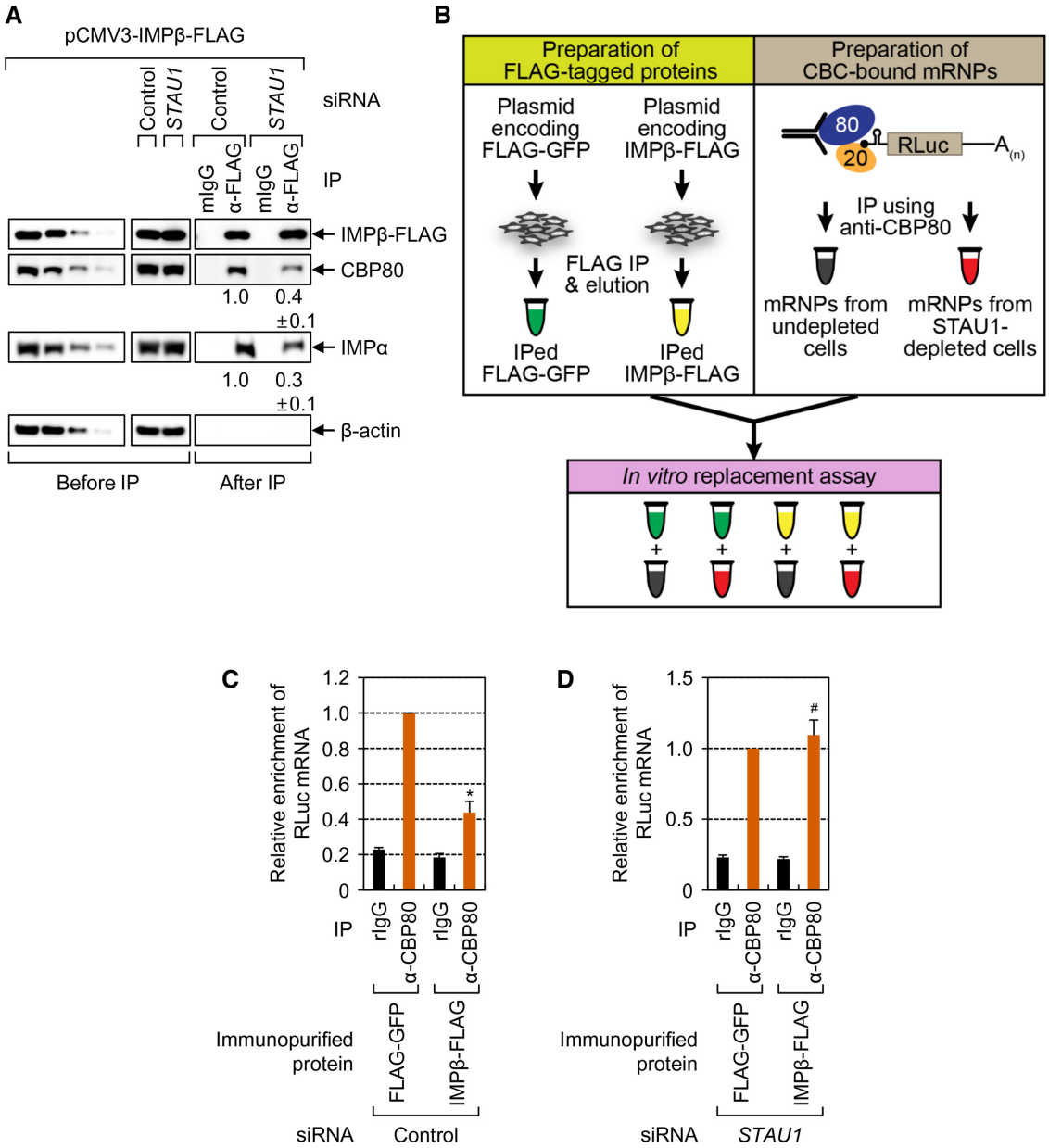

Figure 4. STAU1 promotes an IMPβ-mediated replacement of the CBC by eIF4E *in vivo* and *in vitro*. (**A**) IPs of IMPβ-FLAG in HEK293T cells depleted of STAU1. $n = 3$. (**B–D**) The *in vitro* replacement assay. (B) A schematic diagram of the experimental procedure. For the immunopurification of FLAG-tagged proteins, the extracts of the cells transiently expressing either FLAG-GFP or IMPβ-FLAG were subjected to IPs with anti-FLAG antibody–conjugated agarose beads. The bead-bound FLAG-tagged proteins were eluted by means of 3 × FLAG peptides. For immunopurification of CBC-associated reporter mRNPs, the IPs of endogenous CBP80 were carried out in the extracts of either undepleted or STAU1-depleted cells transiently expressing SL-5′ intron RLuc reporter mRNAs. (C) An *in vitro* replacement assay using reporter mRNPs immunopurified from the undepleted cells. The bead-bound mRNPs were mixed with either immunopurified FLAG-GFP or IMPβ-FLAG. After the reaction, the bead-bound mRNAs were analyzed by qRT-PCRs. $n = 5$; *, $P < 0.05$. (D) An *in vitro* replacement assay involving reporter mRNPs immunopurified from the STAU1-depleted cells. $n = 5$; #, not significant.

S7A–F). Conversely, overexpression of λN-HA-UPF1 or λN-HA-STAU1 decreased or increased the level of eIF4E-associated SL-5′ intron mRNAs, respectively (Supplementary Figure S7A–F). In addition, downregulation of UPF1 or STAU1 respectively decreased or increased the amounts of co-IPed endogenous β-actin and *SMG7* mRNAs with a marginal effect on replication-dependent histone mRNA (*HIST2H2AA3* mRNA; Supplementary Figure S7G–I), which forms a stable CBC-associated mRNP complex via direct interactions between CBP80 and CTIF and between CTIF and stem-loop-binding protein (42). All these data suggest that the UPF1- or STAU1-modulated replacement of CBP80 by eIF4E is a general mechanism behind the regulation of gene expression.

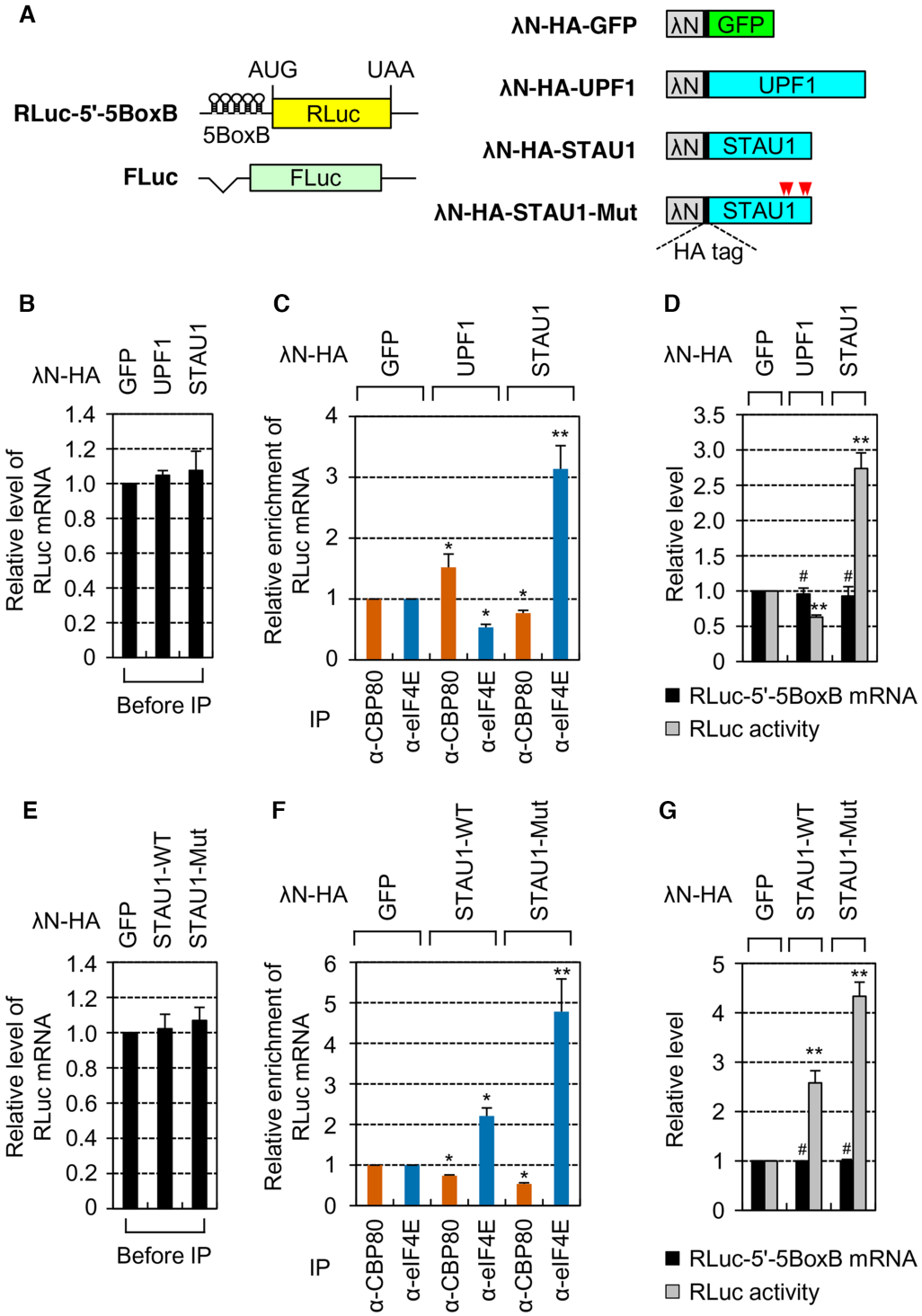

Figure 5. Tethered STAU1 or UPF1 respectively promotes or inhibits the replacement**.** (**A**) A schematic diagram of reporter mRNAs and effectors for tethering experiments with the λN-5BoxB system. A plasmid RLuc-5′-5BoxB reporter contained five tandem repeats of a BoxB sequence (5BoxB) in the 5′UTR. An FLuc-expressing plasmid, pCI-FLuc, served as a reference plasmid. AUG and UAA denote a translation initiation codon and termination codon, respectively. Four residues for single point mutations in STAU1 are indicated by arrowheads in red. (**B**–**D**) Tethering experiments with effector proteins. HEK293T cells were transiently cotransfected with a reporter plasmid, an FLuc reference plasmid and one of the effector plasmids. Total-cell extracts were separated into a nuclear fraction and cytoplasmic fraction. The IPs of endogenous CBP80 or eIF4E were performed in the cytoplasmic fractions. Co-IPed RLuc and FLuc mRNAs were analyzed by qRT-PCRs. $n = 2$; *, $P < 0.05$; **, $P < 0.01$. (B) The influence of the effector proteins on steady-state levels of RLuc reporter mRNAs before IPs. The levels of RLuc mRNAs before IPs were normalized to those of FLuc mRNAs before IPs. (C) Relative levels of co-IPed RLuc mRNAs after IPs. The levels of co-IPed RLuc mRNAs were normalized to co-IPed FLuc mRNAs. Then, the normalized levels in the cells expressing λN-HA-GFP were arbitrarily set to 1.0. (D) The impact of the tethered proteins on translation efficiency. Relative amounts and translation efficiency of the reporter mRNA were measured by qRT-PCR and the dual luciferase assay in the cytoplasmic fractions before IPs. $n = 3$; **, $P < 0.01$; #, not significant. (**E**–**G**) Tethering experiments with λN-HA-STAU1-WT and -Mut. As performed in panels B–D, except that either λN-HA-STAU1-WT or -Mut was tethered. $n = 3$; *, $P < 0.05$; **, $P < 0.01$; #, not significant.

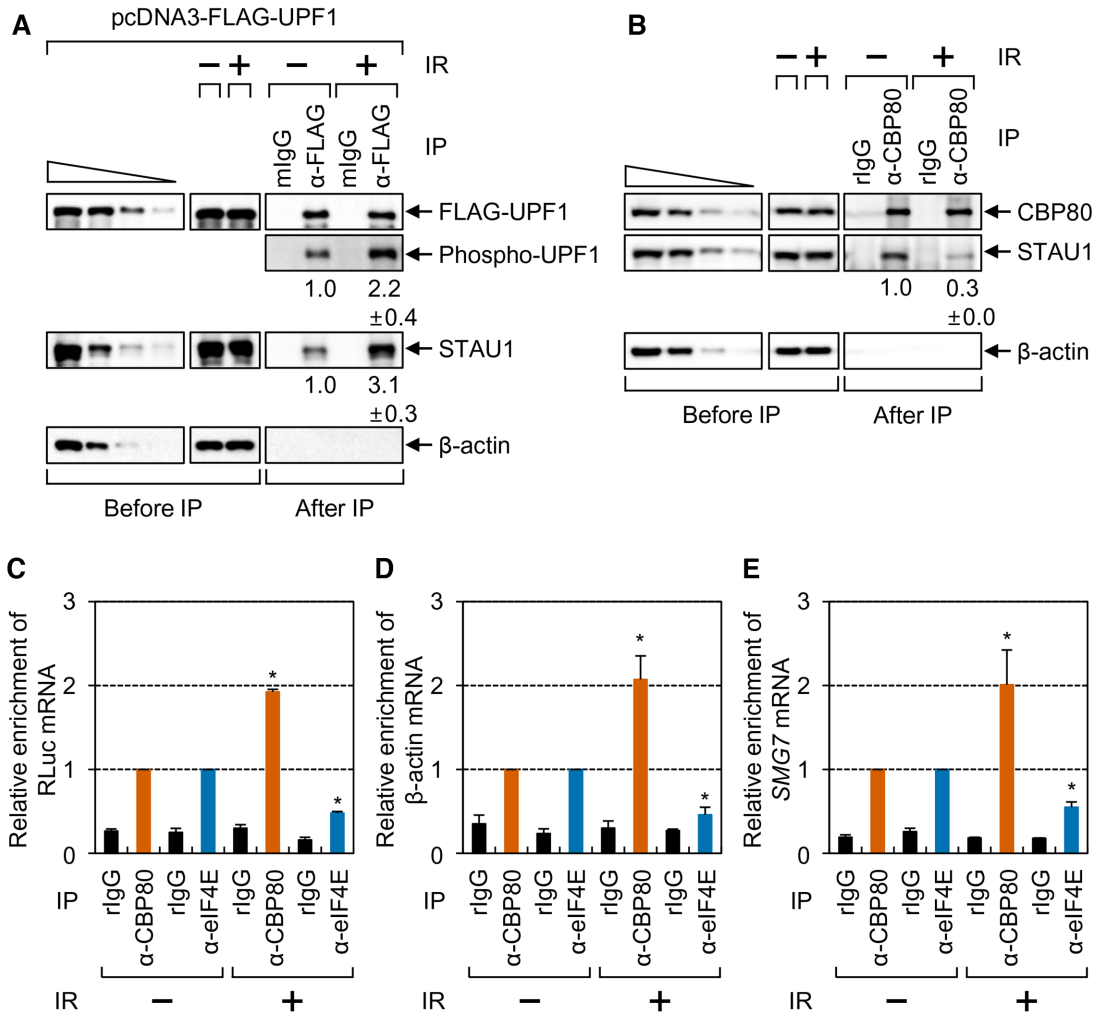

Figure 6. Increased association between UPF1 and STAU1 after IR exposure inhibits the replacement of the CBC by eIF4E. (**A**) The effect of IR exposure on the interaction between UPF1 and STAU1. HEK293T cells transiently expressing FLAG-UPF1 were either untreated or exposed to IR. After cell fractionation, the cytoplasmic extracts were subjected to IPs using either nonspecific mouse IgG (mIgG) or the anti-FLAG antibody; $n = 3$. The intensities of the bands were quantitated and normalized to those of immunoprecipitated FLAG-UPF1. (**B**) The effect of IR exposure on the interaction between CBP80 and STAU1. As performed in panel A, except that the cytoplasmic extracts were subjected to IPs with the anti-CBP80 antibody. $n = 3$. (**C**–**E**) The effect of IR exposure on the replacement. HEK293T cells expressing an SL-5′ intron mRNA were either untreated or exposed to IR. Then, the cytoplasmic extracts were subjected to IPs with the anti-CBP80 antibody, anti-eIF4E antibody, or nonspecific rIgG. After IPs, equal amounts of *in vitro*-synthesized FLuc RNAs were added to the immunoprecipitated samples as a spike-in. $n = 3$; *, $P < 0.05$. (**C**) Relative levels of co-IPed SL-5′ intron mRNA. The levels of co-IPed SL-5′ intron mRNA were normalized to those of FLuc RNAs. The normalized levels of co-IPed SL-5′ intron mRNAs in the IPs of either CBP80 or eIF4E in untreated cells were arbitrarily set to 1.0. (**D**) Relative levels of co-IPed endogenous β-actin mRNAs. The levels of β-actin mRNAs were normalized to those of 18S rRNAs. (**E**) Relative levels of co-IPed endogenous *SMG7* mRNAs. The levels of *SMG7* mRNAs were normalized to those of 18S rRNAs.

UPF1 hyperphosphorylated during IR exposure strongly binds to STAU1 and consequently inhibits the replacement of the CBC by eIF4E

It is well known that (i) UPF1 more strongly interacts with STAU1 when UPF1 is hyperphosphorylated (36), and (ii) IR triggers UPF1 hyperphosphorylation (46). Therefore, we investigated whether IR exposure influences the interaction between UPF1 and STAU1 via UPF1 hyperphosphorylation and thereby the efficiency of the CBC replacement by eIF4E.

Under our experimental conditions, the activation of cellular signaling by IR exposure was evidenced by an increase in both the steady-state level and phosphorylation (at serine 15) of endogenous p53 (Supplementary Figure S8A) (47,48). In addition, IR exposure increased UPF1 hyperphosphorylation by 2.2-fold and the association between UPF1 and STAU1 by 3.1-fold (Figure 6A). Furthermore, IR exposure caused an ∼70% reduction in the amount of co-IPed STAU1 in the IP of CBP80 (Figure 6B). Under the same conditions, exogenously expressed RLuc reporter mRNA, endogenous β-actin mRNA, and endogenous *SMG7* mRNA, the levels of which did not significantly change during IR exposure (Supplementary Figure S8B–D), were found to be more enriched (1.9-, 2.1- and 2.0-fold,

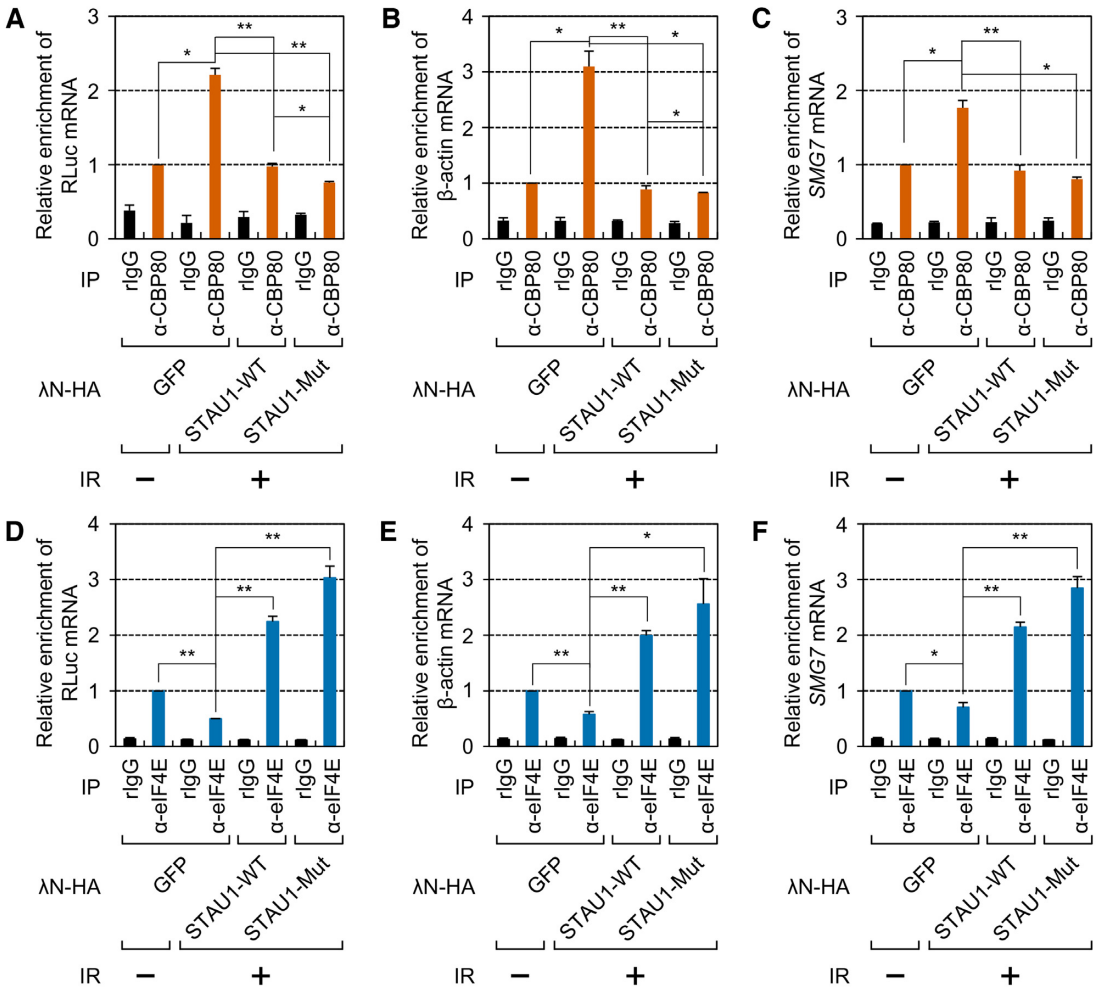

Figure 7. Inhibition of CBC replacement by eIF4E after IR exposure is reversed by STAU1 overexpression. (**A**–**C**) The effect of overexpressed STAU1-WT or STAU1-Mut on enrichment of mRNAs in CBP80 IPs. HEK293T cells transiently expressing an SL-5′ intron RLuc reporter mRNA and overexpressing λN-HA-GFP, λN-HA-STAU1-WT or λN-HA-STAU1-Mut were either untreated or exposed to IR. Next, the cytoplasmic extracts were subjected to IPs with the anti-CBP80 antibody. After that, the immunoprecipitated samples were spiked with equal amounts of *in vitro*-synthesized FLuc RNA. $n = 3$; *, $P < 0.05$; **, $P < 0.01$. (A) Relative levels of co-IPed reporter mRNAs. (B) Relative levels of co-IPed endogenous β-actin mRNAs. (**C**) Relative levels of co-IPed endogenous *SMG7* mRNAs. (**D**–**F**) The effect of overexpressed STAU1-WT or STAU1-Mut on enrichment of mRNAs in eIF4E IPs. As performed in panels A–C, except that the cytoplasmic extracts were subjected to IPs with the anti-eIF4E antibody.

respectively) in the IP of CBP80 and less enriched (52, 54 and 45%, respectively) in the IP of eIF4E during IR exposure (Figure 6C–E).

We next tested the effect of overexpressed STAU1-WT or STAU1-Mut on the replacement during IR exposure. All the tested co-IPed mRNAs (exogenously expressed RLuc reporter mRNA, endogenous β-actin mRNA and endogenous *SMG7* mRNA) turned out to be significantly enriched in the IP of CBP80 in the cytoplasmic extracts of IR-treated cells compared with untreated cells (Figure 7A–C and Supplementary Figure S9A–C). Of note, steady-state levels of the tested mRNAs before IPs did not significantly change after IR exposure (Supplementary Figure S9D–F). On the other hand, smaller amounts of co-IPed mRNAs were found to be enriched in the IP of eIF4E (Figure 7D–F and Supplementary Figure S9G–J). The observed results in each IP were almost completely reversed by overexpression of either λN-HA-STAU1-WT or λN-HA-STAU1-Mut (Figure 7A–F).

Next, we tested whether the change in the replacement efficiency during IR exposure was reflected in the change in global translation efficiency. The latter was assessed by the SUnSET assay, a method allowing for monitoring of newly synthesized proteins by Western blotting with an anti-puromycin antibody. The data from the SUnSET assay (Supplementary Figure S10A) and RLuc reporter mRNAs (Supplementary Figure S10B) revealed that the replacement efficiency correlated with global translation efficiency. In line with these data, global translation efficiency also diminished when the replacement was inhibited by STAU1 downregulation (Supplementary Figure S10C). Collectively, all these findings prompted us to conclude that under the stressful conditions induced by IR exposure, UPF1 becomes hyperphosphorylated and more strongly associates with STAU1, thereby inhibiting the CBC replace-

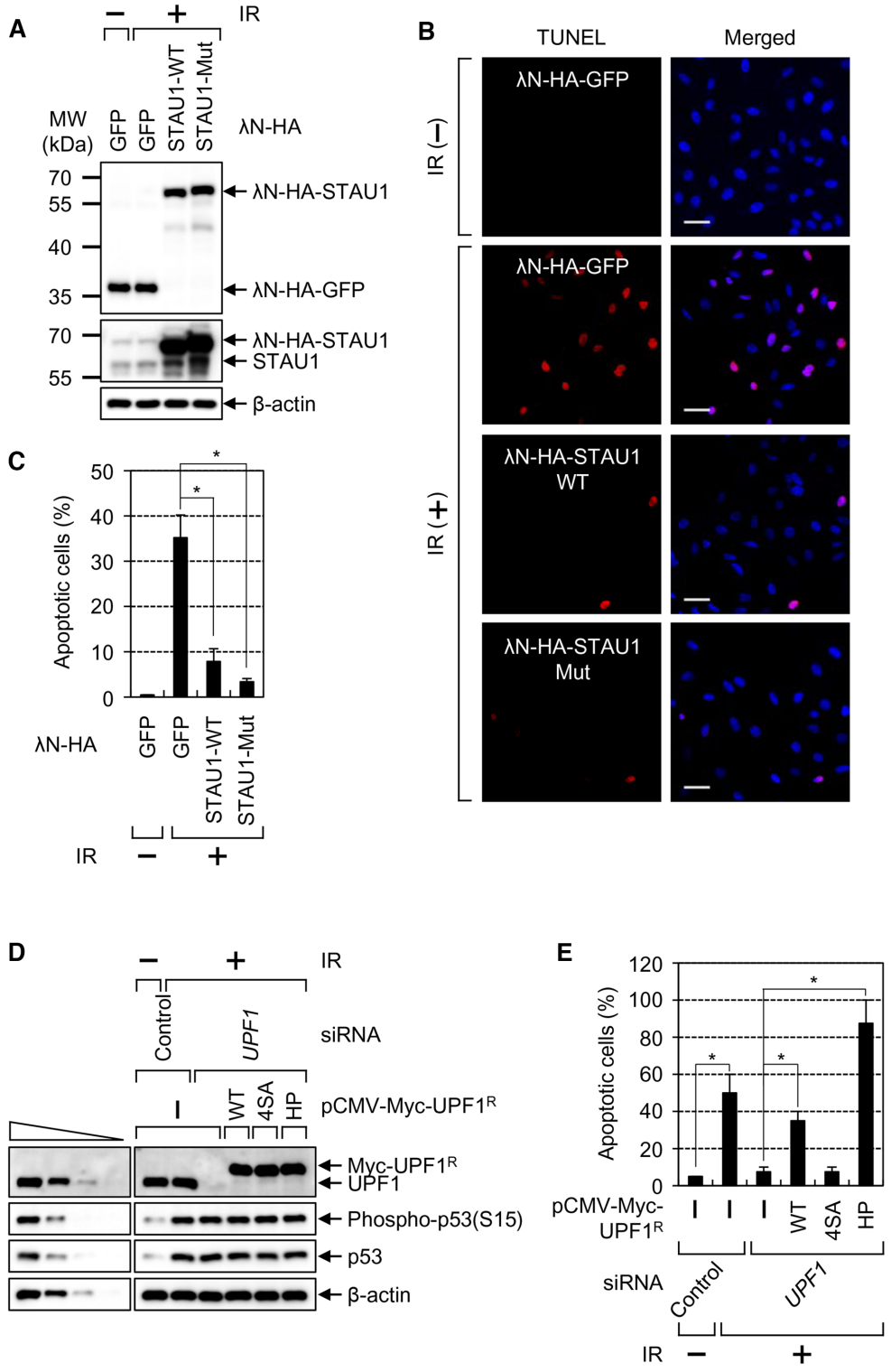

Figure 8. IR-induced apoptosis is significantly inhibited by increased CBC replacement by eIF4E via either STAU1 overexpression or UPF1 downregulation. (**A**–**C**) The TUNEL assay for monitoring IR-induced apoptosis. HeLa cells transiently overexpressing λN-HA-GFP, λN-HA-STAU1-WT or λN-HA-STAU1-Mut were either untreated or exposed to IR and then analyzed by the TUNEL assay. (A) Western blots revealing comparable expression of λN-GFP, λN-STAU1-WT or λN-STAU1-Mut. (B) Representative images of the TUNEL assay. Scale bar, 50 μm. (C) Quantitation of apoptotic cells. The stained cells (apoptotic cells) were counted, and the ratios are presented as a percentage (%). $n = 3$; *, $P < 0.05$. (**D** and **E**) The complementation experiment with siRNA-resistant UPF1. HeLa cells either undepleted or depleted of endogenous UPF1 were transiently transfected with a plasmid expressing Myc-UPF1^R-WT, -4SA or -HP. Then, the cells were either not treated or exposed to IR. (D) Western blots revealing specific downregulation and comparable expression of Myc-UPF1^R-WT or mutant relative to the level of endogenous UPF1. (E) Quantitation of apoptotic cells. The stained cells (apoptotic cells) were counted, and the ratios are presented as a percentage (%). $n = 2$; *, $P < 0.05$.

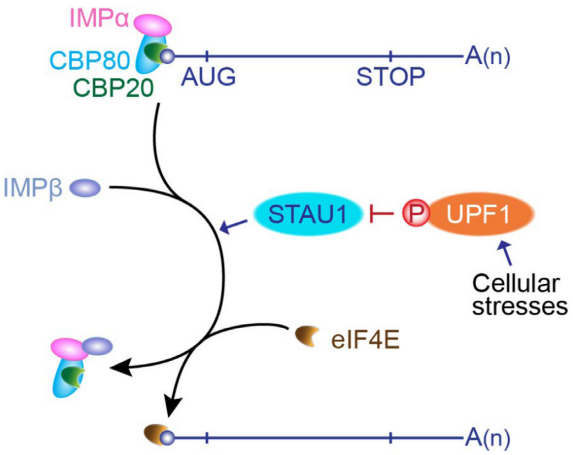

Figure 9. The proposed model of the replacement of the CBC by eIF4E. STAU1 serves as a positive regulator of the replacement by facilitating an interaction between the CBC–IMPα complex and IMPβ. Under stress conditions, UPF1 becomes hyperphosphorylated and the replacement is inhibited via increased association between STAU1 and hyperphosphorylated UPF1. The circled P indicates a phosphate group. See the 'Discussion' section for details.

ment by eIF4E and concomitantly suppressing global translation.

The apoptosis induced by IR exposure inversely correlates with the efficiency of the CBC replacement by eIF4E

Considering that IR exposure causes apoptosis (49,50), we investigated whether the observed inhibition of CBC replacement by eIF4E is accompanied by IR-induced apoptosis. Under our conditions, the population of apoptotic cells was increased from baseline to ∼35% by IR exposure (Figure 8A–C). The observed increase was reversed to 8 or 3% by overexpression of λN-HA-STAU1-WT or λN-HA-STAU1-Mut, respectively. In support of the inhibitory role of UPF1 in the CBC replacement by eIF4E, we clearly demonstrated that overexpressed λN-HA-STAU1-Mut had a stronger effect than did overexpressed λN-HA-STAU1-WT. Of note, the levels of endogenous SMD substrates (*c-JUN* mRNA, *IL7R* mRNA and *SERPINE1* mRNAs) were not significantly changed by IR exposure and overexpression of STAU1 (Supplementary Figure S11), ruling out the possibility that the reverse effects observed in Figures 6–8 may be due to a change in SMD efficiency.

The observed IR-induced apoptosis and inhibition of the CBC replacement by eIF4E were next corroborated by complementation experiments with the depletion of HeLa cells of UPF1 and with expression of an siRNA-resistant (R) WT, 4SA (hypophosphorylated), or HP (hyperphosphorylated) form of UPF1 (27,28). The hypophosphorylated UPF1–4SA contains four substitutions (S1073A, S1078A, S1096A and S1116A) of the amino acid residues previously confirmed to be phosphorylated by SMG1 (51,52). UPF1-HP is deficient in ATPase and helicase activities, consequently becoming hyperphosphorylated (51,53,54). The results showed that the apoptosis induced by IR exposure was significantly reduced by UPF1 downregulation. Of note, expression of UPF1-WT or UPF1-HP, but not UPF1–4SA, reversed the observed reduction (Figure 8D and E; Supplementary Figure S12). Together with the observation of IR-induced UPF1 hyperphosphorylation and thus an increased interaction between UPF1 and STAU1 (Figure 6), these data indicate that UPF1 hyperphosphorylated during IR exposure is engaged in the inhibition of the CBC replacement, and therefore, in apoptosis.

DISCUSSION

It is generally thought that the CBC and eIF4E are largely in charge of mRNA surveillance and abundant protein synthesis, respectively. Because (i) CBC-bound mRNAs are precursors of eIF4E-bound mRNAs (13) and (ii) the efficiency of translation driven by the CBC is very weak relative to that driven by eIF4E (6,7), efficient and abundant protein synthesis should be preceded by proper replacement of the CBC by eIF4E. Although this is a crucial step for gene expression, not much is known about molecular details of this replacement. In this study, we provide molecular evidence that STAU1 and UPF1 serve as a positive and negative regulator of the replacement, respectively, where UPF1 inhibits the ability of STAU1 to promote the replacement via a direct interaction between UPF1 and STAU1. Such an interplay between STAU1 and UPF1 for the replacement is partially responsible for the apoptosis induced by IR exposure.

According to our findings, we propose the following model (Figure 9). Newly synthesized mRNAs are exported from the nucleus to cytoplasm via the nuclear pore complex with their 5′-cap structure bound to the CBC. It is known that (i) both UPF1 and STAU1 are predominantly localized to the cytoplasm, but these proteins can shuttle between the nucleus and cytoplasm (18,55–58); (ii) UPF1 binds to mRNAs promiscuously even before translation (17); or, co-transcriptionally associates with nascent RNAs at most of the active transcription sites of Pol II (18); and (iii) STAU1 transiently associates with small and weak hairpin structures (59–61). Therefore, the CBC-bound mRNPs being exported may contain STAU1 and UPF1 that have already associated with CBC-bound mRNPs in the nucleus. Alternatively, the cytosolic STAU1 and UPF1 may be recruited to CBC-bound mRNPs being exported. In this scenario, the local amounts of cytosolic STAU1 and UPF1 could be determined by the number of *cis*-acting elements for binding to STAU1 or UPF1 in CBC-bound mRNPs. Given that STAU1 and UPF1 are complexed with the CBC in a manner that is resistant to RNase A treatment (Figure 3), RNA-independent recruitment of free cytosolic STAU1 or UPF1 may also be possible too as an alternative. In either case, the relative ratio of local amounts of cytosolic STAU1 and UPF1 near CBC-bound mRNPs being exported may determine the efficiency of CBC replacement by eIF4E. When STAU1 is predominant, the STAU1–IMPα–CBC-capped mRNA complex provides a favorable platform for the loading of IMPβ, which triggers mRNA dissociation from the complex. In an opposite case, predominant UPF1 attenuates the ability of STAU1 to promote the replacement, consequently delaying the replacement.

Hyperphosphorylated UPF1 more strongly binds to STAU1. As a consequence, the inhibitory effect of UPF1 on the replacement should be more drastic when UPF1 is hy-

perphosphorylated. Indeed, in our study, we observed that IR exposure promotes UPF1 hyperphosphorylation and the association between UPF1 and STAU1, thereby enhancing the inhibition of CBC replacement by eIF4E (Figure 6). The observed inhibition of the replacement during IR exposure is accompanied by efficient apoptosis (Figure 8). These data are suggestive of plausible participation of UPF1 hyperphosphorylation in the CBC replacement by eIF4E under other stress conditions, where UPF1 becomes hyperphosphorylated by phosphoinositide 3-kinase–related kinases. For instance, when DNA replication is compromised, activated ATR and DNA-PK trigger UPF1 hyperphosphorylation (12,26,62). In addition, genotoxic stresses activate ATM and SMG1, both of which induce UPF1 hyperphosphorylation (12,46). Therefore, considering the ubiquitous expression of STAU1 and UPF1, the regulation of the replacement by STAU1 and UPF1 may not be limited to IR-induced apoptosis. The biological importance of this regulation needs to be determined in future studies.

DATA AVAILABILITY

The QuantSeq 3′-mRNA sequencing data were deposited in the Sequence Read Archive of the National Center for Biotechnology Information under the accession number SRP139879.

SUPPLEMENTARY DATA

Supplementary Data are available at NAR Online.

ACKNOWLEDGEMENTS

We thank Melissa J. Moore for providing the plasmids No intron and 5′ intron, Luc DesGroseillers for the plasmid expressing STAU1^{55}-HA$_3$, and Lynne E. Maquat for the anti-UPF1 antibody and the plasmid expressing STAU1-Mut.

FUNDING

National Research Foundation (NRF) of Korea by the Korean government (Ministry of Science, ICT and Future Planning) [NRF-2015R1A3A2033665]; NRF by the Ministry of Education, Science and Technology [NRF-2017R1D1A1B03034138 to K.J., in part]. Funding for open access charge: NRF of Korea.
Conflict of interest statement. None declared.

REFERENCES

1. Singh,G., Pratt,G., Yeo,G.W. and Moore,M.J. (2015) The clothes make the mRNA: Past and present trends in mRNP fashion. *Annu. Rev. Biochem.*, **84**, 325–354.
2. Muller-McNicoll,M. and Neugebauer,K.M. (2014) Good cap/bad cap: how the cap-binding complex determines RNA fate. *Nat. Struct. Mol. Biol.*, **21**, 9–12.
3. Ramanathan,A., Robb,G.B. and Chan,S.H. (2016) mRNA capping: biological functions and applications. *Nucleic Acids Res.*, **44**, 7511–7526.
4. Gonatopoulos-Pournatzis,T. and Cowling,V.H. (2014) Cap-binding complex (CBC). *Biochem. J.*, **457**, 231–242.
5. Maquat,L.E., Tarn,W.Y. and Isken,O. (2010) The pioneer round of translation: features and functions. *Cell*, **142**, 368–374.
6. Ishigaki,Y., Li,X., Serin,G. and Maquat,L.E. (2001) Evidence for a pioneer round of mRNA translation: mRNAs subject to nonsense-mediated decay in mammalian cells are bound by CBP80 and CBP20. *Cell*, **106**, 607–617.
7. Kim,K.M., Cho,H., Choi,K., Kim,J., Kim,B.W., Ko,Y.G., Jang,S.K. and Kim,Y.K. (2009) A new MIF4G domain-containing protein, CTIF, directs nuclear cap-binding protein CBP80/20-dependent translation. *Genes Dev.*, **23**, 2033–2045.
8. Ryu,I. and Kim,Y.K. (2017) Translation initiation mediated by nuclear cap-binding protein complex. *BMB Rep.*, **50**, 186–193.
9. Brogna,S., McLeod,T. and Petric,M. (2016) The meaning of NMD: translate or perish. *Trends Genet.*, **32**, 395–407.
10. Lykke-Andersen,S. and Jensen,T.H. (2015) Nonsense-mediated mRNA decay: an intricate machinery that shapes transcriptomes. *Nat. Rev. Mol. Cell Biol.*, **16**, 665–677.
11. Kurosaki,T., Popp,M.W. and Maquat,L.E. (2019) Quality and quantity control of gene expression by nonsense-mediated mRNA decay. *Nat. Rev. Mol. Cell Biol.* **20**, 406–420.
12. Kim,Y.K. and Maquat,L.E. (2019) UPFront and center in RNA decay: UPF1 in nonsense-mediated mRNA decay and beyond. *RNA*, **25**, 407–422.
13. Lejeune,F., Ishigaki,Y., Li,X. and Maquat,L.E. (2002) The exon junction complex is detected on CBP80-bound but not eIF4E-bound mRNA in mammalian cells: dynamics of mRNP remodeling. *EMBO J.*, **21**, 3536–3545.
14. Sato,H., Hosoda,N. and Maquat,L.E. (2008) Efficiency of the pioneer round of translation affects the cellular site of nonsense-mediated mRNA decay. *Mol. Cell*, **29**, 255–262.
15. Hosoda,N., Kim,Y.K., Lejeune,F. and Maquat,L.E. (2005) CBP80 promotes interaction of Upf1 with Upf2 during nonsense-mediated mRNA decay in mammalian cells. *Nat. Struct. Mol. Biol.*, **12**, 893–901.
16. Hwang,J., Sato,H., Tang,Y., Matsuda,D. and Maquat,L.E. (2010) UPF1 association with the cap-binding protein, CBP80, promotes nonsense-mediated mRNA decay at two distinct steps. *Mol. Cell*, **39**, 396–409.
17. Zund,D., Gruber,A.R., Zavolan,M. and Muhlemann,O. (2013) Translation-dependent displacement of UPF1 from coding sequences causes its enrichment in 3′ UTRs. *Nat. Struct. Mol. Biol.*, **20**, 936–943.
18. Singh,A.K., Choudhury,S.R., De,S., Zhang,J., Kissane,S., Dwivedi,V., Ramanathan,P., Petric,M., Orsini,L., Hebenstreit,D. *et al.* (2019) The RNA helicase UPF1 associates with mRNAs co-transcriptionally and is required for the release of mRNAs from gene loci. *Elife*, **8**, e41444.
19. Kim,Y.K., Furic,L., Desgroseillers,L. and Maquat,L.E. (2005) Mammalian Staufen1 recruits Upf1 to specific mRNA 3′UTRs so as to elicit mRNA decay. *Cell*, **120**, 195–208.
20. Gong,C. and Maquat,L.E. (2011) lncRNAs transactivate STAU1-mediated mRNA decay by duplexing with 3′ UTRs via Alu elements. *Nature*, **470**, 284–288.
21. Park,E. and Maquat,L.E. (2013) Staufen-mediated mRNA decay. *Wiley Interdiscip. Rev. RNA*, **4**, 423–435.
22. Heraud-Farlow,J.E. and Kiebler,M.A. (2014) The multifunctional Staufen proteins: conserved roles from neurogenesis to synaptic plasticity. *Trends Neurosci.*, **37**, 470–479.
23. Thomas,M.G., Martinez Tosar,L.J., Desbats,M.A., Leishman,C.C. and Boccaccio,G.L. (2009) Mammalian Staufen 1 is recruited to stress granules and impairs their assembly. *J. Cell Sci.*, **122**, 563–573.
24. Nott,A., Meislin,S.H. and Moore,M.J. (2003) A quantitative analysis of intron effects on mammalian gene expression. *RNA*, **9**, 607–617.
25. Choe,J., Ryu,I., Park,O.H., Park,J., Cho,H., Yoo,J.S., Chi,S.W., Kim,M.K., Song,H.K. and Kim,Y.K. (2014) eIF4AIII enhances translation of nuclear cap-binding complex-bound mRNAs by promoting disruption of secondary structures in 5'UTR. *Proc. Natl. Acad. Sci. U.S.A.*, **111**, E4577–E4586.
26. Choe,J., Ahn,S.H. and Kim,Y.K. (2014) The mRNP remodeling mediated by UPF1 promotes rapid degradation of replication-dependent histone mRNA. *Nucleic Acids Res.*, **42**, 9334–9349.
27. Isken,O., Kim,Y.K., Hosoda,N., Mayeur,G.L., Hershey,J.W. and Maquat,L.E. (2008) Upf1 phosphorylation triggers translational repression during nonsense-mediated mRNA decay. *Cell*, **133**, 314–327.

28. Park,O.H., Park,J., Yu,M., An,H.T., Ko,J. and Kim,Y.K. (2016) Identification and molecular characterization of cellular factors required for glucocorticoid receptor-mediated mRNA decay. *Genes Dev.*, **30**, 2093–2105.
29. Cho,H., Park,O.H., Park,J., Ryu,I., Kim,J., Ko,J. and Kim,Y.K. (2015) Glucocorticoid receptor interacts with PNRC2 in a ligand-dependent manner to recruit UPF1 for rapid mRNA degradation. *Proc. Natl. Acad. Sci. U.S.A.*, **112**, E1540–E1549.
30. Cho,H., Kim,K.M. and Kim,Y.K. (2009) Human proline-rich nuclear receptor coregulatory protein 2 mediates an interaction between mRNA surveillance machinery and decapping complex. *Mol. Cell*, **33**, 75–86.
31. Cho,H., Han,S., Park,O.H. and Kim,Y.K. (2013) SMG1 regulates adipogenesis via targeting of staufen1-mediated mRNA decay. *Biochim. Biophys. Acta*, **1829**, 1276–1287.
32. Gleghorn,M.L., Gong,C., Kielkopf,C.L. and Maquat,L.E. (2013) Staufen1 dimerizes through a conserved motif and a degenerate dsRNA-binding domain to promote mRNA decay. *Nat. Struct. Mol. Biol.*, **20**, 515–524.
33. Park,J., Park,Y., Ryu,I., Choi,M.H., Lee,H.J., Oh,N., Kim,K., Kim,K.M., Choe,J., Lee,C. *et al.* (2017) Misfolded polypeptides are selectively recognized and transported toward aggresomes by a CED complex. *Nat. Commun.*, **8**, 15730.
34. Park,O.H., Ha,H., Lee,Y., Boo,S.H., Kwon,D.H., Song,H.K. and Kim,Y.K. (2019) Endoribonucleolytic cleavage of m(6)A-Containing RNAs by RNase P/MRP complex. *Mol. Cell*, **74**, 494–507.
35. Ryu,I., Won,Y.S., Ha,H., Kim,E., Park,Y., Kim,M.K., Kwon,D.H., Choe,J., Song,H.K., Jung,H. *et al.* (2019) eIF4A3 phosphorylation by CDKs affects NMD during the cell cycle. *Cell Rep.*,**26**, 2126–2139.
36. Cho,H., Kim,K.M., Han,S., Choe,J., Park,S.G., Choi,S.S. and Kim,Y.K. (2012) Staufen1-mediated mRNA decay functions in adipogenesis. *Mol. Cell*, **46**, 495–506.
37. Schmidt,E.K., Clavarino,G., Ceppi,M. and Pierre,P. (2009) SUnSET, a nonradioactive method to monitor protein synthesis. *Nat. Methods*, **6**, 275–277.
38. Bustin,S.A., Benes,V., Garson,J.A., Hellemans,J., Huggett,J., Kubista,M., Mueller,R., Nolan,T., Pfaffl,M.W., Shipley,G.L. *et al.* (2009) The MIQE guidelines: minimum information for publication of quantitative real-time PCR experiments. *Clin. Chem.*, **55**, 611–622.
39. Langmead,B. and Salzberg,S.L. (2012) Fast gapped-read alignment with Bowtie 2. *Nat. Methods*, **9**, 357–359.
40. Quinlan,A.R. and Hall,I.M. (2010) BEDTools: a flexible suite of utilities for comparing genomic features. *Bioinformatics*, **26**, 841–842.
41. Furic,L., Maher-Laporte,M. and DesGroseillers,L. (2008) A genome-wide approach identifies distinct but overlapping subsets of cellular mRNAs associated with Staufen1- and Staufen2-containing ribonucleoprotein complexes. *RNA*, **14**, 324–335.
42. Choe,J., Kim,K.M., Park,S., Lee,Y.K., Song,O.K., Kim,M.K., Lee,B.G., Song,H.K. and Kim,Y.K. (2013) Rapid degradation of replication-dependent histone mRNAs largely occurs on mRNAs bound by nuclear cap-binding proteins 80 and 20. *Nucleic Acids Res.*, **41**, 1307–1318.
43. Sato,H. and Maquat,L.E. (2009) Remodeling of the pioneer translation initiation complex involves translation and the karyopherin importin beta. *Genes Dev.*, **23**, 2537–2550.
44. Dias,S.M., Wilson,K.F., Rojas,K.S., Ambrosio,A.L. and Cerione,R.A. (2009) The molecular basis for the regulation of the cap-binding complex by the importins. *Nat. Struct. Mol. Biol.*, **16**, 930–937.
45. Izaurralde,E., Lewis,J., Gamberi,C., Jarmolowski,A., McGuigan,C. and Mattaj,I.W. (1995) A cap-binding protein complex mediating U snRNA export. *Nature*, **376**, 709–712.
46. Brumbaugh,K.M., Otterness,D.M., Geisen,C., Oliveira,V., Brognard,J., Li,X., Lejeune,F., Tibbetts,R.S., Maquat,L.E. and Abraham,R.T. (2004) The mRNA surveillance protein hSMG-1 functions in genotoxic stress response pathways in mammalian cells. *Mol. Cell*, **14**, 585–598.
47. Banin,S., Moyal,L., Shieh,S., Taya,Y., Anderson,C.W., Chessa,L., Smorodinsky,N.I., Prives,C., Reiss,Y., Shiloh,Y. *et al.* (1998) Enhanced phosphorylation of p53 by ATM in response to DNA damage. *Science*, **281**, 1674–1677.
48. Canman,C.E., Lim,D.S., Cimprich,K.A., Taya,Y., Tamai,K., Sakaguchi,K., Appella,E., Kastan,M.B. and Siliciano,J.D. (1998) Activation of the ATM kinase by ionizing radiation and phosphorylation of p53. *Science*, **281**, 1677–1679.
49. Caelles,C., Helmberg,A. and Karin,M. (1994) p53-dependent apoptosis in the absence of transcriptional activation of p53-target genes. *Nature*, **370**, 220–223.
50. Symonds,H., Krall,L., Remington,L., Saenz-Robles,M., Lowe,S., Jacks,T. and Van Dyke,T. (1994) p53-dependent apoptosis suppresses tumor growth and progression in vivo. *Cell*, **78**, 703–711.
51. Durand,S., Franks,T.M. and Lykke-Andersen,J. (2016) Hyperphosphorylation amplifies UPF1 activity to resolve stalls in nonsense-mediated mRNA decay. *Nat. Commun.*, **7**, 12434.
52. Kashima,I., Yamashita,A., Izumi,N., Kataoka,N., Morishita,R., Hoshino,S., Ohno,M., Dreyfuss,G. and Ohno,S. (2006) Binding of a novel SMG-1-Upf1-eRF1-eRF3 complex (SURF) to the exon junction complex triggers Upf1 phosphorylation and nonsense-mediated mRNA decay. *Genes Dev.*, **20**, 355–367.
53. Kurosaki,T., Li,W., Hoque,M., Popp,M.W., Ermolenko,D.N., Tian,B. and Maquat,L.E. (2014) A post-translational regulatory switch on UPF1 controls targeted mRNA degradation. *Genes Dev.*, **28**, 1900–1916.
54. Lee,S.R., Pratt,G.A., Martinez,F.J., Yeo,G.W. and Lykke-Andersen,J. (2015) Target discrimination in nonsense-mediated mRNA decay requires Upf1 ATPase activity. *Mol. Cell*, **59**, 413–425.
55. Shi,M., Zhang,H., Wang,L., Zhu,C., Sheng,K., Du,Y., Wang,K., Dias,A., Chen,S., Whitman,M. *et al.* (2015) Premature termination codons are recognized in the nucleus in A Reading-Frame dependent manner. *Cell Discov.*, **1**. 15001.
56. Azzalin,C.M., Reichenbach,P., Khoriauli,L., Giulotto,E. and Lingner,J. (2007) Telomeric repeat containing RNA and RNA surveillance factors at mammalian chromosome ends. *Science*, **318**, 798–801.
57. Azzalin,C.M. and Lingner,J. (2006) The human RNA surveillance factor UPF1 is required for S phase progression and genome stability. *Curr. Biol.*, **16**, 433–439.
58. Martel,C., Macchi,P., Furic,L., Kiebler,M.A. and Desgroseillers,L. (2006) Staufen1 is imported into the nucleolus via a bipartite nuclear localization signal and several modulatory determinants. *Biochem. J.*, **393**, 245–254.
59. Sugimoto,Y., Vigilante,A., Darbo,E., Zirra,A., Militti,C., D¢Ambrogio,A., Luscombe,N.M. and Ule,J. (2015) hiCLIP reveals the in vivo atlas of mRNA secondary structures recognized by Staufen 1. *Nature*, **519**, 491–494.
60. de Lucas,S., Oliveros,J.C., Chagoyen,M. and Ortin,J. (2014) Functional signature for the recognition of specific target mRNAs by human Staufen1 protein. *Nucleic Acids Res.*, **42**, 4516–4526.
61. Ricci,E.P., Kucukural,A., Cenik,C., Mercier,B.C., Singh,G., Heyer,E.E., Ashar-Patel,A., Peng,L. and Moore,M.J. (2014) Staufen1 senses overall transcript secondary structure to regulate translation. *Nat. Struct. Mol. Biol.*, **21**, 26–35.
62. Kaygun,H. and Marzluff,W.F. (2005) Regulated degradation of replication-dependent histone mRNAs requires both ATR and Upf1. *Nat. Struct. Mol. Biol.*, **12**, 794–800.